

DEVELOPMENT OF LIFE PREDICTIVE METHODS ON NOVALT16 COMBUSTOR WITH SIMPLIFIED PHYSICS BASED MODELS

Federico Funghi

Federico.funghi@bhge.com
Baker Hughes, a GE company (BHGE)
Via Matteucci, 2 – Firenze (IT)

Michele Provenzale

Michele.provenzale@bhge.com
Baker Hughes, a GE company (BHGE)
Via Matteucci, 2 – Firenze (IT)

ABSTRACT

Simplified physics based models are becoming increasingly important in the Oil and Gas industry, especially in the framework of life prediction methods. The use of these analytically lean models is primarily driven by the adoption of digital twin paradigm within the industry but it's also pushed ahead by design or manufacturing related issues, such as the need of supporting new product introduction more promptly, or expediting the resolution of the RCA's. The study presented herein reports a description of methods and models used to create the life prediction platform of NovaLT16 combustor liners. Simplified thermal models have been developed, tuned against test data and then used to predict the temperature distribution on liners as a function of the machine actual operating conditions. Following the definition of the most critical area on the outer liner in terms of durability, a stress model of that location has been also created, providing the primary input for the LCF and crack growth models. All these models, in series, had given sound support for the combustor development and can be also easily connected to remote diagnostic and asset management systems to predict the durability of the liners as a function of gas turbine operating parameters.

INTRODUCTION

Within the framework of recent digital twin paradigm, analytical and numerical models are assuming an increasing importance, especially for what concerns predictive maintenance related issues. Intervals to perform gas turbine (GT) maintenance could be modified in accordance to the actual operating profile of any single specific machine, thus allowing a more flexible usage of the equipment for sake of customers' productivity and economic return.

The introduction and development of this new paradigm is associated with the creation of lifing models capable of predicting parts durability as a function of machine operating conditions. As of today however,

models developed during the design phase, which could be used with this scope, are usually limited to a single operating configuration, typically the worst, in such a way to ensure the life requirements are met for the most severe condition the GT is subjected to.

Creating models capable of predicting life for different operating conditions could be very time consuming, in consideration of the effort required to define, set up, execute and repeat a full set of aero, heat transfer and structural analyses.

In order to overcome this limitation, a lateral approach is proposed herein, which, to some extent, makes uses of simplified physics based models, capable of reducing the computation time required to analyze a GT full operational envelope, and thus allowing the adoption of the new paradigm. More flexible and lean models would also be very useful in other product development phases, such as product testing, off design conditions evaluation, GT introductory stage and initial RCA's. In all of these cases, the use of lean models capable of promptly predicting the structural response of the system would surely speed up the development process or the issue resolution.

One other important business aspect which could also act in driving the adoption of lean lifing models is the potential interest of a number of customers to develop internal predictive capabilities on their fleets, leveraging this new technology.

The background considerations above paved the way for the development and the implementation of the approach with lean durability models on the NovaLT16 annular combustion chamber.

NOMENCLATURE

AFR:	Air to fuel ratio
BHGE:	Baker Hughes, a GE company
BHM:	Bayesian Hybrid Modelling
c:	Specific heat capacity
C _i :	Thermal resistance 'i' due to convection

d:	distance between locations of T_{min} and T_{max}
DACRS :	Dual Annular Counter Rotating Swirler
DLE:	Dry Low Emission
DT th:	Through thickness temperature difference
E:	Young modulus of the material
FAR	Full Annular Rig
FETT:	First Engine To Test
FSFL:	Full Speed Full Load
FSNL:	Full Speed No Load
f_{ps} :	pilot fuel burner split
GT:	Gas Turbine
HCF:	High Cycle Fatigue
HT:	Hold Time
K:	Stress intensity factor
Kc:	Fracture toughness
Kth:	Threshold stress intensity factor
K_{eff} :	Effective stress intensity factor
k:	Material conductivity / Ramberg-Osgood constant
K_f :	Fatigue notch factor
LCF:	Low Cycle Fatigue
m:	Walker exponent
n:	Ramberg-Osgood constant
N_i :	Crack nucleation life
N_p :	Crack propagation life
OL:	Outer Liner
P_{CD} :	Compressor discharge air pressure
RCA:	Root Cause Analysis
R_i :	Thermal resistance 'i' due to radiation
RM&D:	Remote Monitoring and Diagnostics
R_{sq-adj} :	R squared adjusted
S:	Linear elastic stress
SS:	Steady State
TBC:	Thermal Barrier Coating
T_{CD} :	Compressor discharge air temperature
TF:	Transfer Function
T_g :	Gas temperature
T_{in} :	Metal temperature at instrumentation hole, hot side
T_m :	Metal temperature
T_{max} :	Max outer liner metal temperature
T_{min} :	Min outer liner metal temperature
T_{nh} :	High-pressure turbine velocity
T_{out} :	Metal temperature at instrumentation hole, cold side
α :	Coefficient of thermal expansion
ΔP :	Delta pressure across combustor
$\Delta \epsilon$:	Delta strain
$\Delta \sigma$:	Delta stress
ϵ :	Strain
σ :	Stress
σ_3 :	Minimum principal stress
ρ :	Mass density

1. BACKGROUND

Annular combustors (Figure 1.1) are typically made of two annular liners, one dome, a set of fuel nozzles, heat shields and, in most cases, one or more baffles. The two liners are usually connected to a shaped ring (the dome) on combustor forward side and define the boundaries of flame containment. Dome and liners forward side are protected from hot flame by heat shields, commonly supported by the dome itself. Baffles are used for either fluid dynamic reasons (to create a gap with liners for proper combustor cooling) or structural reasons (stiffening/damping support), and sometimes for both [6].

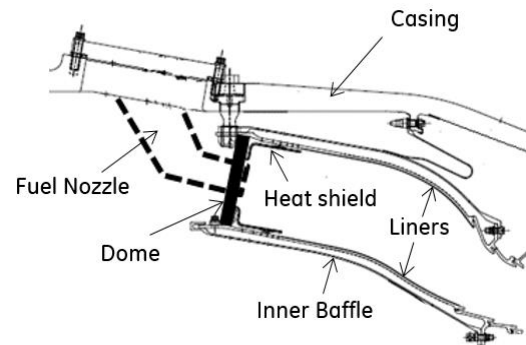


Figure 1.1. Sketch of NovaLT16 combustor cross section

The NovaLT16 GT has a DLE annular combustor, which is equipped with 39 burners. A selective fuel injection control system feeds the burners in accordance to the engine operating conditions. From engine start-up to approximately 40% load not all the burners are fed, but just a fraction of them, while all 39 burners are on when the 40% load limit is overcome (fuel staging).

The fuel burner design is based on Dual Annular Counter Rotating Swirler (DACRS) technology [7], widely employed by GE for aero-derivative stationary gas turbines. A schematic of the baseline burner geometry is shown in Figure 1.2. It involves two main separate fuel circuits, pilot and premix. The fuel from premix circuit is injected radially inward into the airstream at the swirler location and produces a homogeneous mixture at premixer duct exit. The pilot nozzles fuel injection, located at the burner tip, allows a proper flame anchoring in the combustor volume downstream the premixers.

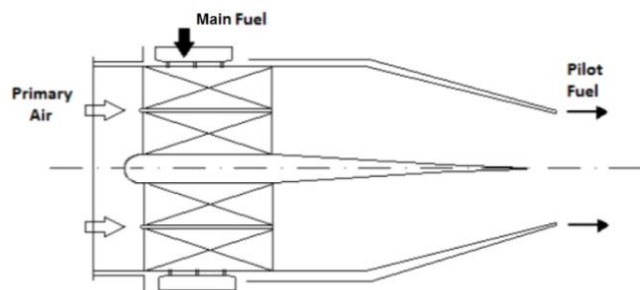


Figure 1.2. DACRS fuel burner scheme

2. REFERENCE FE MODELS OF THE COMBUSTOR

A full set of thermal structural models of the combustion chamber were developed during the design phases, providing the stress distribution and the LCF life on all combustor components. This initial reference models, together with the results coming from FETT and Endurance tests on NovaLT16 allowed to define the critical areas (in terms of LCF/HCF strength and/or displacements) where to apply the simplified physics based models approach.

This reference model was used to capture thermal structural behavior of the system also during the fuel staging phases. Fuel staging allows to sustain the flame at partial load conditions, when a few burners are left off. In this configuration the combustor sees a circumferential variation of its metal temperatures, passing from sections where burners are on to sections with burners off.

Although this temperature gradient could generate some additional stresses in the structure, it has been demonstrated by analysis that this contribution is negligible, as well as its impact on LCF life. For this reason, the effect of burner staging has been not considered in this study.

Figure 2.1 shows a typical metal temperature distribution on the outer liner assumed during the design stage. Analyses revealed that the liners were structurally very robust overall, the only possible critical areas being the instrumentation holes of the outer liner (if subjected to off design temperatures). Actually Tests performed on the combustion chamber also aimed at investigating the structural response of the outer liner in the region of instrumentation holes.

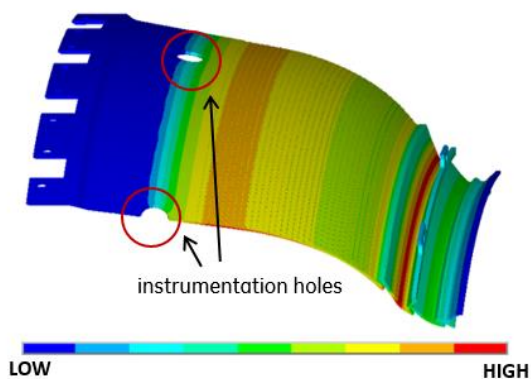


Figure 2.1. Typical temperature distribution on NovaLT16 outer liner.

3. NOVALT16 TEST OUCOMES

A large amount of test data was acquired during the development of the NovaLT16 GT which have also been

used to create and validate the simplified physics based thermal model of the combustion chamber.

The entire set of data comes from three different test campaigns:

- 1) Test performed on a full scale annular combustor rig to assess emissions, blow-out and flashback resistance (FAR);
- 2) Test performed on the full engine, with a wide set of instrumentation systems, for a complete mechanical assessment (FETT);
- 3) Continuous endurance test up to 8000 hours for a reliability assessment (FETT Endurance).

The full-scale annular combustor test rig (FAR), installed in SestaLab test cell (Radicondoli, Italy), has been designed with the aim of replicating different ambient and operative conditions of the gas turbine, by independently varying combustion air flow, temperature, pressure and fuel flow. The combustion chamber included the inlet diffuser and the outlet nozzle throat, and replicated the full-scale geometry from the real gas turbine [2]. In Figure 3.1 a cross section of the rig is represented.

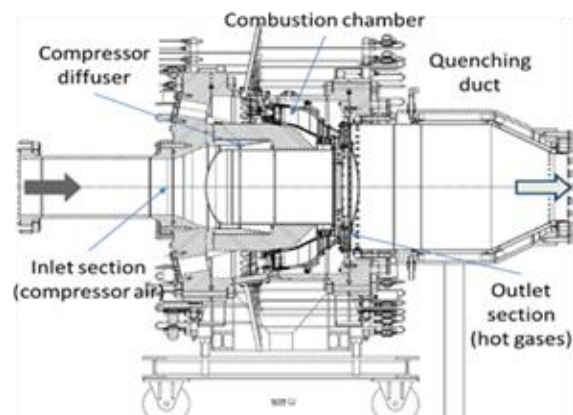


Figure 3.1. Full Annular Rig main features

Both test campaigns on the engine (FETT and FETT Endurance) were performed on a newly created test rig (Figure 3.2) specifically for the NovaLT16, that had been built at the BHGE facility in Florence, Italy.

The test bed was composed of:

- a filter house and four inlet air measurement tubes which allows an excellent accuracy in air flow rate measurement,
- a complete production-standard gas turbine enclosure, baseplate, inlet duct and exhaust stack,
- a complete production-standard auxiliaries enclosure and baseplate,
- a braking system made by a synchronous electric generator,
- a load gearbox which connects the gas turbine to the electric generator.

Natural gas was available from the national public grid and its composition was continuously monitored by a gas-chromatographer.

During the FETT test campaign, the gas turbine was equipped with over 2,200 direct measurement points, covering flange-to-flange, package and auxiliaries. This massive instrumentation allowed to investigate and validate all the engine working conditions, in terms of flows, metal temperatures, dynamic stresses, combustor dynamic pulsations, performance and emissions [1].



Figure 3.2. NovaLT16 FETT test cell

With regard to the combustion system instrumentation, during all the three test campaigns both inner and outer liner were instrumented with 24 thermocouples each. The thermocouples have been installed in 6 axial and 4 circumferential locations (Figure 3.3), and measure the metal temperature of the external (cold) liner surface.

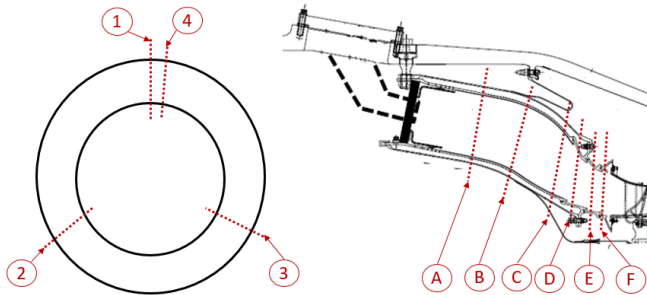


Figure 3.3. Combustion Chamber metal temperature layout schematic

A lot of information on combustor operation and structural behavior was acquired during the test campaigns, which allowed to achieve a robust validation of the numerical models used all along the design phases.

Tests also confirmed that for off design conditions a slight cracking occurred on the outer liner instrumentation hole, which was expected from preliminary structural assessment.

4. SIMPLIFIED PHYSICS BASED MODELS OF NOVALT16 COMBUSTOR LINERS

Following preliminary analysis indications and test outcomes, a thermal structural model of outer liner instrumentation hole cracking has been developed, which considered a wide operating envelope of the machine, including off design conditions.

The diagram below shows the model creation strategy and the information flow of the hole cracking.

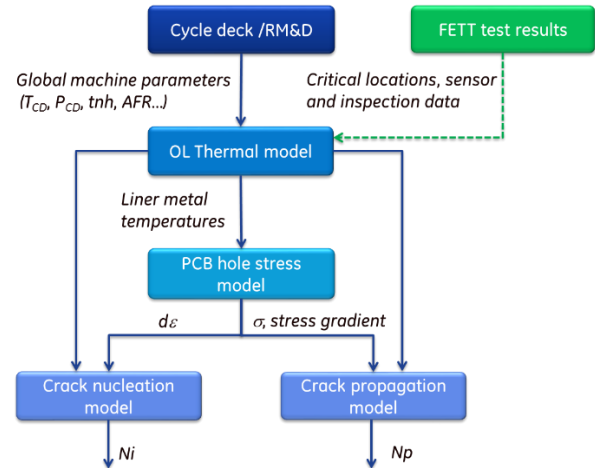


Figure 4.1. Simplified physics based models of outer liner instrumentation hole – flow diagram

The thermal model gives the metal temperature distribution on the outer liner as a function of the global operating parameters of the machine, from start up to steady state condition to shut down. Data coming from FETT instrumentation have been fused with physical relations and used to create a semi-empirical model of the temperature distribution at liner thermocouple locations.

Temperature distribution, together with the delta pressure across the combustor (which is also a global parameter of the machine and varies along the mission), are then used as input for the stress/strain model. Next, data coming from both stress/strain and thermal model feed a LCF (low cycle fatigue) model that predicts the crack initiation life at the hole edge. Finally, a crack growth analysis is carried out, which computes the life (in cycles) to reach the max allowable crack length, after which a disruptive propagation could jeopardize the combustor functionality or structural integrity.

5. THERMAL MODEL

The thermal model of the liners has been created to respond to the following requirements:

- predicting the distribution of liner metal temperature with a sufficient accuracy,
- making use of the input parameters only that are monitored through GT standard instrumentation,

- predicting the liner temperature distribution under transient conditions, not only at steady state operation, since the failure mechanisms of some critical liner locations depend on the metal temperature variation over time.

Due to the constraints above, the thermal model has been based on a semi-empirical approach that involves the main physical parameters affecting the gas temperature on liner hot and cold side (air to fuel ratio, burner fuel split, compressor discharge air temperature). High-pressure turbine shaft speed has been considered as input, and a delay parameter has been also added to account for liner thermal inertia.

Depending on the fuel burner staging strategy, the distribution of the gas temperature inside the combustion chamber is not axisymmetric when the load is under 40% of FSFL condition. In fact, at partial load, the liner will see a circumferential variation of the metal temperature from regions with hotter gas temperature (hot arch) to regions with lower gas temperature (cold arch), while above 40% of FSFL condition, the circumferential temperature distribution is fully axisymmetric.

Detailed 3D thermal-structural models have shown the circumferential temperature distribution has only secondary effects on the LCF life of liners, and for this reason the simplified thermal model presented herein is axisymmetric, which means that it is capable of predicting the metal temperature distribution in the ‘hot arch’ region.

The model has been used to compute the metal temperature in each one of the 6 liner axial locations (A, B, C, D, E, F in Figure 3.3) which were monitored with thermocouples during test. The model coefficients have been opportunely tuned in each axial location of inner and outer liner, to match the thermocouple readings. Finally, a cubic spline interpolation has been used to predict the metal temperature distribution on the entire axial length of the two liners.

The model structure to compute the liner metal temperature in a generic axial location ‘i’ and at the instant ‘t’ is:

$$Tm_i(t) = k_i \cdot f_1(tnh(t)) \cdot f_2(f_{ps}(t)) \cdot \frac{T_{cd}(t)}{T_{cd}^*} \cdot \frac{AFR^*}{AFR(t)} \quad (1)$$

where:

$$f_1(tnh(t)) = a_i \cdot e^{b_i(tnh(t)-tnh^*)} \quad (2)$$

$$f_2(f_{ps}(t)) = c_i \cdot (f_{ps}(t) - f_{ps}^*) + d_i \quad (3)$$

and:

$$\begin{aligned} tnh(t) &: \text{high-pressure turbine velocity} \\ f_{ps}(t) &: \text{pilot fuel burner split} \\ T_{cd}(t) &: \text{compressor discharge air temperature} \\ AFR(t) &: \text{air to fuel ratio} \end{aligned}$$

that are directly retrieved from the engine Data Acquisition System

while:

$$\begin{aligned} tnh^* &: \text{reference high-pressure turbine velocity} \\ f_{ps}^* &: \text{reference pilot fuel burner split} \\ T_{cd}^* &: \text{reference compressor discharge air temp} \\ AFR^* &: \text{reference air to fuel ratio} \end{aligned}$$

are reference constants.

All of the above are defined as global operating parameters, while k_i, a_i, b_i, c_i, d_i are the tuning constants in the generic axial location ‘i’.

AFR is the air to fuel ratio scaled to a single fed fuel burner according to the following formula:

$$AFR = \frac{\text{compressor inlet air mass flow}}{\text{total fuel mass flow}} \cdot \frac{n_b}{39} \quad (4)$$

where n_b is the number of the actual burners on.

The constants k_i, a_i, b_i, c_i, d_i have been opportunely tuned on several transient and steady state conditions, from engine start-up up to full load, by minimizing the error with respect to the average value of the four thermocouples measurements in each of the six axial locations. During the staging phases, only the thermocouples in the hot arch have been selected for temperature averaging.

The validation of the thermal model has been performed on a different set of data, which includes transient (start-up, loading and fast loading, unloading, shut-down, loads steps, load rejections) and steady state (full speed no load, partial load, full speed full load) conditions.

The model has shown an accuracy of $\pm 35^\circ\text{C}$ on the metal temperature prediction during the transient conditions and $\pm 20^\circ\text{C}$ at steady state, with respect to the average value of the thermocouples readings, which was judged to be acceptable for the scope of this study.

In Figure 5.1 a comparison at one axial location between predicted and measured metal temperature of outer liner during a transient start-up and loading is shown.

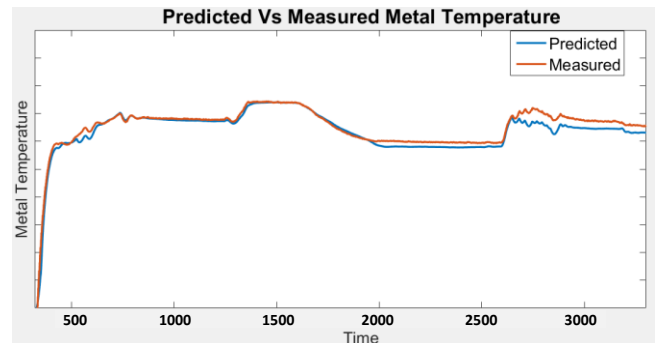


Figure 5.1. OL Predicted and measured metal temperature comparison

The thermal model, as shown in the pages above, is able to compute liner temperature distribution on the external (cold) surface. In order to calculate the temperature distribution on the internal (hot) side a further simplified thermal model has been defined, according to the scheme in Figure 5.2.

A 1D thermal model has been considered to simulate the heat transfer from hot to cold side, assuming the conduction to occur through the thickness only. Actually, given the cold side temperature distribution, a small in-plane conduction could be present as well, especially at the hole, but it has been demonstrated to be negligible with respect to the first order effects due to through thickness conduction.

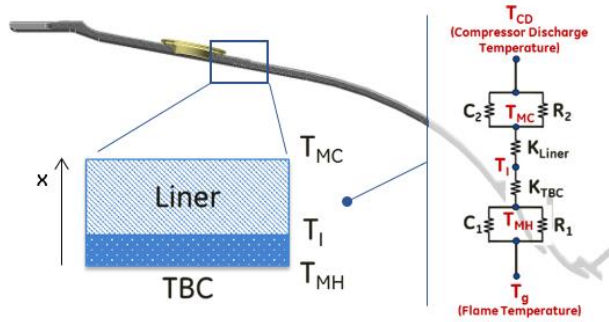


Figure 5.2. 1D thermal model of through thickness conduction

In the figure above, T_{MC} is the metal temperature on the cold side, which is the output of the primary thermal model. The 1D thermal model computes $T(x)$ as a function of:

- C_1 : convection Gas \rightarrow Liner
- R_1 : radiation Gas \rightarrow Liner
- C_2 : convection Liner \rightarrow Baffle
- R_2 : radiation Liner \rightarrow Baffle
- K_{TBC} : conductivity of TBC
- K_{Liner} : conductivity of liner
- T_g : temperature of hot gas
- T_{CD} : gas temperature of compressor discharge

and time, in accordance to the heat equation (for both TBC and liner base material):

$$-\frac{\partial}{\partial x} k \frac{\partial T(x,t)}{\partial x} = \rho c \frac{\partial T(x,t)}{\partial t} \quad (5)$$

where ρ = density, k = conductivity, c = specific heat capacity (all of the previous are function of temperature), T = temperature (function of t and x), t = time, x = through thickness distance (as in Figure 5.2).

The thermal parameters C_1 , C_2 , R_1 , R_2 are obtained from global operating parameters (see above) using characteristic heat transfer formulas, some of which are BHGE proprietary knowledge, while some others can be easily found in literature. k_{TBC} and k_{Liner} are material conductivities, T_{CD} is itself a global operating parameter. T_{MH} is calculated as a function of time at each liner axial station, given T_{MC} and the thermal parameters, by solving the heat equation with finite difference methods.

6. LIFING MODELS OF OUTER LINER INSTRUMENTATION HOLE

The life assessment of outer liner instrumentation hole respectively comprises, in series:

- A stress analysis
- An LCF analysis
- A crack propagation analysis

FE models used for the structural assessment consists of a sector model of 20° centered around the hole, as shown in the picture below.

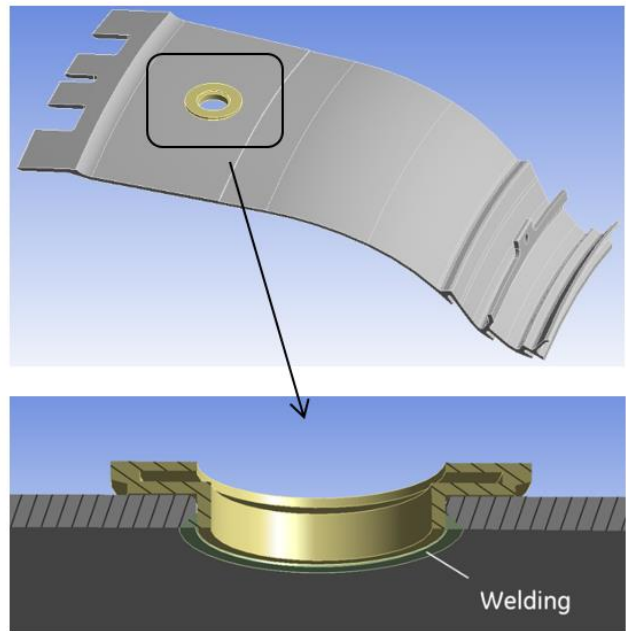


Figure 6.1. FE structural model of the OL around the instrumentation hole

At the instrumentation hole the liner is welded to a support ring which houses a ferrule whose function is to limit the air leakage into the combustor. Both the ferrule ring and the weld joint region are explicitly simulated.

Since the physical problem has a circumferential symmetry, the use of a 20° sector model is sufficient to get a good degree of accuracy. However, a slight asymmetry in the circumferential temperature distribution is actually present within the chamber, being the liner metal temperatures slightly lower in the section comprised between two adjacent burners, but it has been

demonstrated, by the analysis performed on the FE reference model, that this difference has no appreciable impact on durability, since the circumferential temperature gradients are more than one order of magnitude lower than the axial gradients. The choice not to model the circumferential temperature gradient in the simplified model introduces an error of about 2% on LCF life, which is judged to be acceptable.

Figure 6.2 shows the direction of the crack propagation as found during FETT inspection.

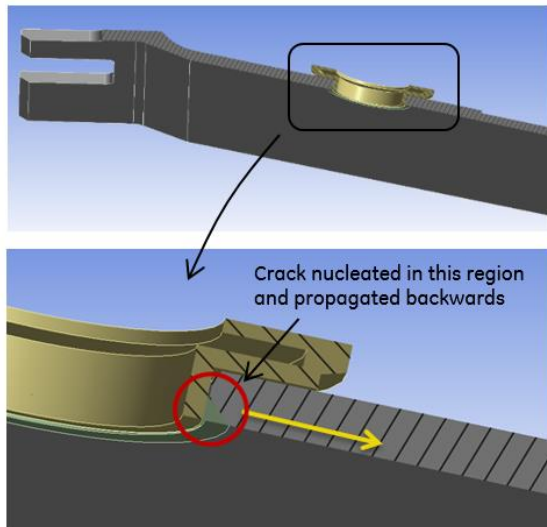


Figure 6.2. Crack growth direction

FE model simplification with respect to the global reference model allows to run multiple cases within short time, which is paramount in this kind of assessment.

7. STRESS MODEL

The outer liner is subjected both thermal and mechanical loads. The latter are basically referred to the pressure difference across the combustion chamber which varies along the mission. Pressure difference is lower at partial load and higher at FSFL. Thermally generated stresses are due to the temperature gradient across the liner thickness and to the in-plane temperature difference around the hole.

The stress model has been created by considering both mechanical and thermal contributions, according to the scheme of Figure 7.1.

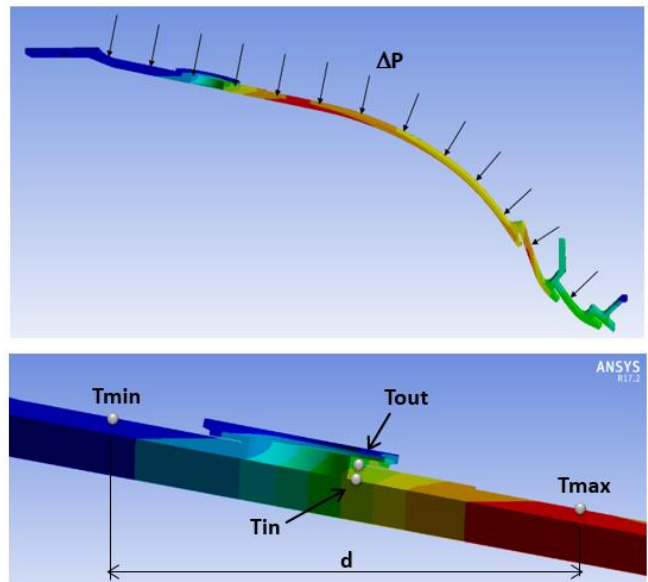


Figure 7.1. Input parameters of structural runs

Linear elastic stress field has been solved for the three different external loads separately (ΔP , through thickness temperature gradient, in-plane temperature gradient). In this way the relative weight of the three contributions on the overall stress level is captured, as well as an insight on the physical mechanisms acting on the system.

The effect of the through thickness gradient on the stress field is captured by solving the system for different combinations of ‘ T_{out} ’ (temperature of liner external surface at the backward hole edge) and ‘ T_{in} ’ (temperature of liner internal surface at the backward hole edge), as shown in Figure 7.1.

The effect of the in-plane temperature difference is included in the stress field computation for a number of combinations of ‘ T_{max} ’ (temperature peak on the liner, outer side), ‘ T_{min} ’ (lowest temperature on the liner, outer side) and ‘ d ’ (minimum axial distance between T_{min} and T_{max}).

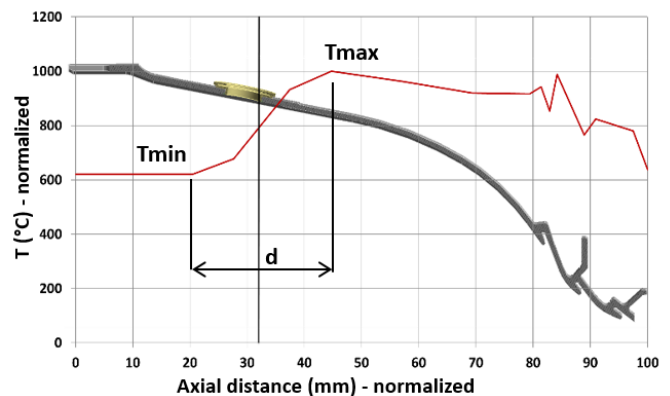


Figure 7.2. Typical metal temperature distribution on outer liner – distances and temperatures are normalized

7.1 LINEAR ELASTIC MODEL

The linear stress tensor (for all the combinations of delta pressure, through thickness gradient and in-plane gradient) is computed on four points at the back edge of the instrumentation hole, as shown in the picture below and the most critical one is considered for the LCF assessment.

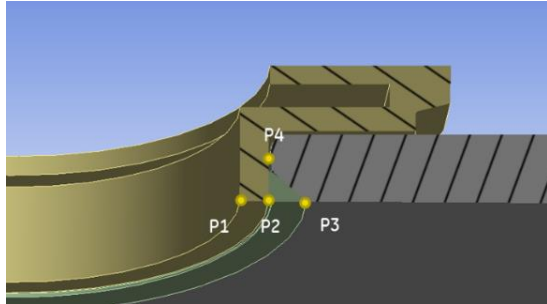


Figure 7.3. Stress control points

It was shown from preliminary analysis that the critical locations for all the conditions considered are point P1 and P2, where the stresses are locally uniaxial (along the hoop direction at the back edge), and always compressive during operating condition, as per picture below. Although the stress is generally higher at P1, point P2 could be actually more critical due to the presence of welding.

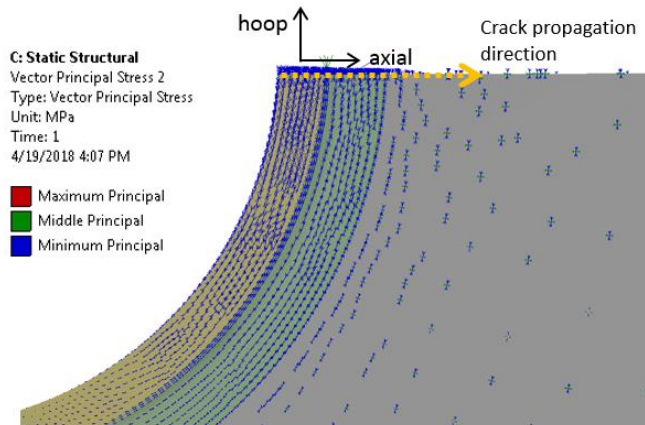


Figure 7.4. Principal stress distribution around the instrumentation hole (internal side, back edge) due to thermal or mechanical load – stress is compressive and locally uniaxial

Since the stress is uniaxial in the region of interest, the stress model can be simplified, replacing the stress tensor with just one of its components, the minimum principal stress (σ_3).

The values of σ_3 at P1 and P2 can be calculated for each of external load contributions and expressed in the form below:

$$\sigma_3 = d_0 \Delta P + d_1 \alpha E (T_{in} - T_{out}) + f(T_{min}, T_{max}, d) \quad (6)$$

where: ΔP =delta pressure across the combustor, α =coefficient of thermal expansions of liner material, E =young modulus of liner material, d_0, d_1 =coefficients of the first two terms

The first term of equation (6) represents the contribution to the overall hole stress due to the delta pressure, the second term refers to the stress due to through thickness temperature gradient and the last term is a function of the in-plane delta temperature.

The first two terms in the equation are linear. The third term has a more complex form and has been determined by running a series of structural analyses in accordance to a full factorial DOE space.

The resulting TF (Transfer Function) of σ_3 due to in-plane delta temperature has been computed using a Bayesian Hybrid Modelling (BHM) approach [4], [9]. This method, implemented in GE proprietary statistical tools, allowed to reach a very good accuracy ($R_{sq-adj} = 99.9\%$) in predicting the stress at the instrumentation hole.

Figure below shows a graphical representation of σ_3 due to all the input parameters.

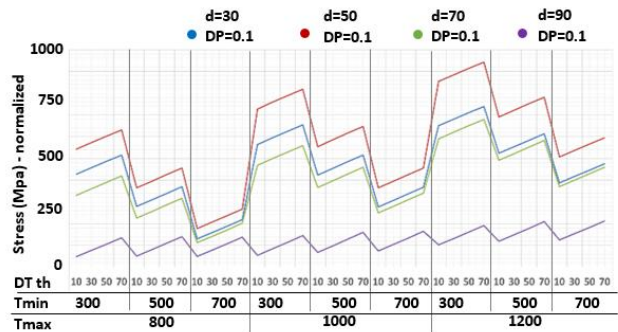


Figure 7.5. Graphical representation of σ_3 TF

The following figure reports the relative weight of the input parameters on overall hole stress.

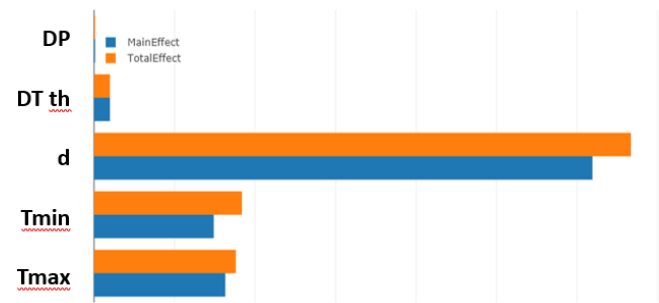


Figure 7.6. Relative weight of input parameters on instrumentation hole stress

In the graph above, the ‘MainEffect’ refers to the first order contribution from the input variable on the output. The ‘TotalEffect’ shows the combined effect the input

variable has on the output (2-way interaction, 3-way, and higher order too).

The axial distance between Tmax and Tmin (d) is the parameter with the highest weight on the TF, followed by the absolute values of Tmax and Tmin. The contribution due to DP is negligible and the stress due to through thickness temperature gradient is at least one order of magnitude less intense than the stress caused by the primary effects.

At the time this study was performed ‘d’ had been defined with some amount of uncertainty, due to the difficulty of measuring the temperature gradient just after the heat shield. Next refined heat transfer assessments had indicated this distance with better accuracy.

The other parameters are directly obtained as input from the thermal model (Tmin, Tmax, Tout, Tin) and from the machine control system or RM&D (ΔP).

7.2 ELASTIC PLASTIC MODEL

Elastic stress, computed by following what reported in the previous chapter, have been converted to elastic-plastic stress in accordance to Glinka Model [8].

This model has been demonstrated to be applicable to cases with local material plasticization. Test cases carried out within BHGE revealed that Glinka method works fine for thermally induced stresses too, and produces better results than the more widely used Neuber approach.

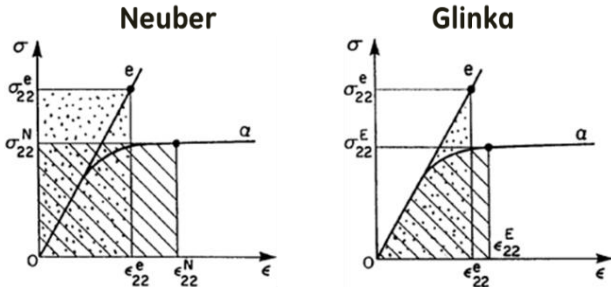


Figure 7.7. Comparison Neuber vs Glinka methods to compute plastic stress and strain

Glinka method has been used to compute the elastic plastic stress (σ), the stress range (dσ) and the strain range (dε) between the critical timesteps of the GT mission profile, in accordance to the formulas below [8].

$$\frac{\sigma^2}{E} + \frac{2\sigma}{n+1} \left(\frac{\sigma}{K}\right)^{\frac{1}{n}} = \frac{(K_f S)^2}{E} \quad (7)$$

$$\frac{\Delta\sigma^2}{E} + \frac{4\Delta\sigma}{n+1} \left(\frac{\Delta\sigma}{2K}\right)^{\frac{1}{n}} = \frac{(K_f \Delta S)^2}{E} \quad (8)$$

$$\Delta\epsilon = \frac{\Delta\sigma}{E} + 2 \left(\frac{\Delta\sigma}{2K}\right)^{\frac{1}{n}} \quad (9)$$

where ‘K_f’ is the fatigue notch factor, ‘S’ is the elastic stress, ‘k’ and ‘n’ are the Ramberg-Osgood constants of the material cyclic stress-strain curve, function of temperature. It has been demonstrated that the delta strain computed with the Glinka method is well aligned with the FE results obtained with a full elastic plastic analysis for one mission profile.

As a sample, Figure 7.8 shows the minimum principal stress (σ₃) at the instrumentation hole critical location as a function of the time, for one of the typical mission profile extracted from FETT test cases. Values are normalized.

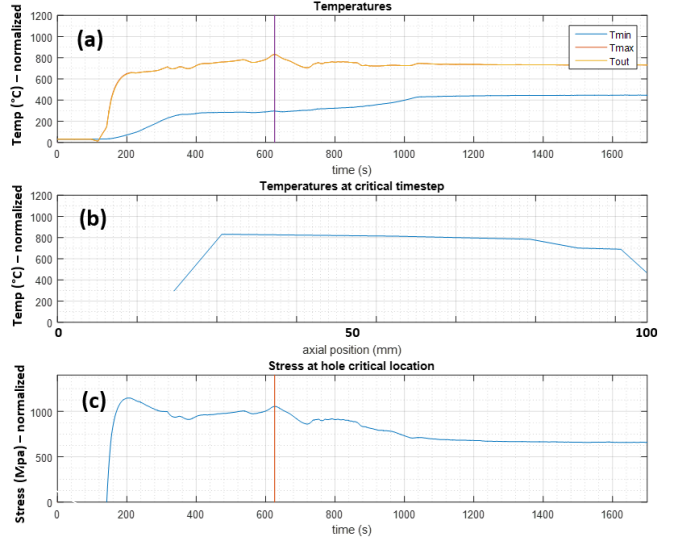


Figure 7.8. (a) Temperature profiles along the time on the control locations (Tmax, Tmin, Tout) – (b) temperature profile along the outer liner curvilinear abscissa – (c) minimum principal stress profile along the time at the instrumentation hole edge. All parameters are normalized.

8. LCF MODEL

The highest Δε along the mission profile, computed as per previous chapter, is used as input to determine the LCF life of the outer liner at the instrumentation hole.

BHGE internal proprietary LCF curves have been used, with 5 hours hold time. The hold time is the time of permanence at operating temperature during one start up – shut down cycle and accounts for the effects of creep damage in the crack nucleation. Interaction LCF-Creep is therefore addressed by making use of the LCF curves with HT. A sample set of normalized LCF curves for outer liner material is shown below. Mean stress effects are also accounted for.

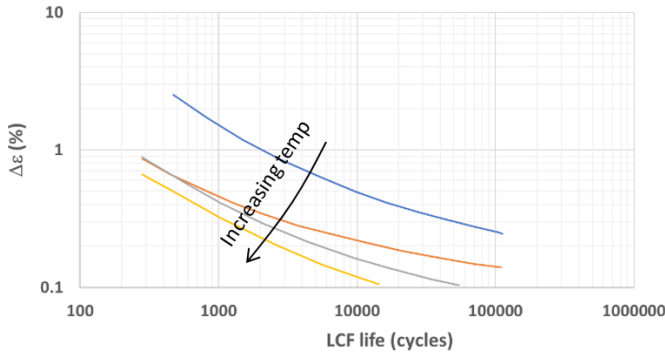


Figure 8.1. Sample of LCF curves with HT – from BHGE proprietary material database. $\Delta\epsilon$ is normalized

LCF model revealed that the crack initiation life is aligned with the FETT outcomes, where off design metal temperatures were reached in some circumstances. In fact, the crack at instrumentation hole originated after few hundreds of start up – shut down cycles, which well matches with the life estimation computed by the LCF model. The model also indicated that, within the normal GT design operating envelope, no LCF issues on the hole are expected.

Overall, the durability model developed herein has the advantage to be able to predict the life degradation rate for a very wide operating envelope, thus providing an estimation of the damage evolution also for partial load states, for instance, where life consumption is low, or for off design conditions as well, which impact life much more severely.

9. CRACK PROPAGATION MODEL

A crack propagation model has been also developed in this lifing framework. The scope is predicting the crack growth rate for different operating conditions.

Crack propagation analysis has been performed using a BHGE proprietary tools. Input for crack growth assessment involve three aspects: geometry, material properties and loading.

Geometrical features are: crack type (e.g. through thickness, corner crack), initial crack length, thickness, width and length of the equivalent plate which simulates the actual liner dimensions. These parameters have been defined in accordance to what shown in Figure 9.1.

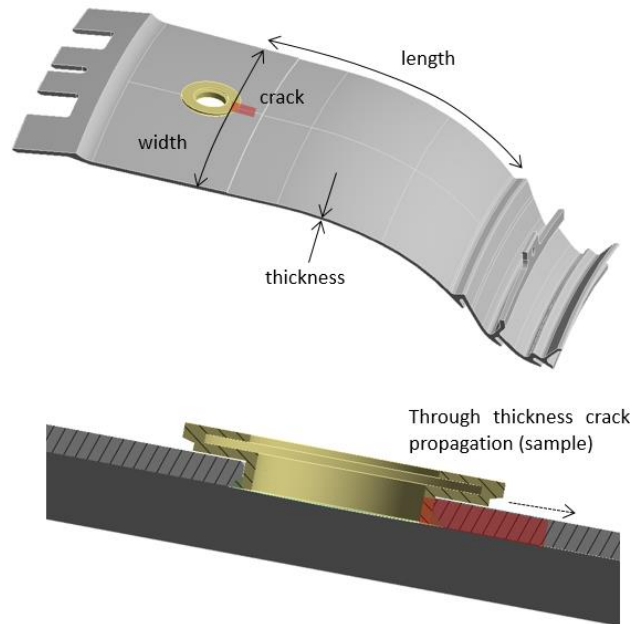


Figure 9.1. Geometrical definition of the equivalent plate for crack growth assessment

Material properties for crack propagation are expressed in terms of Paris curves, at different temperatures, extracted from BHGE material database (Figure 9.2).

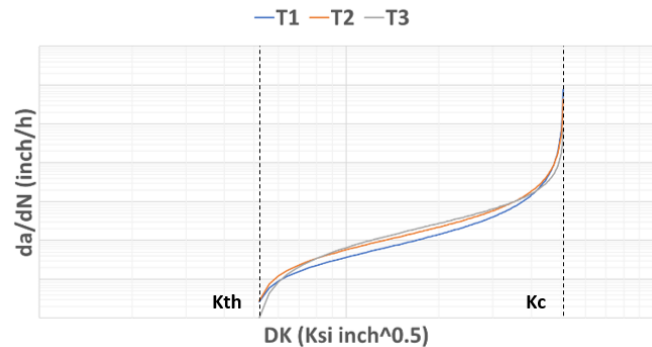


Figure 9.2. Paris curves of liner material in the temperature range of interest. K_{th} = threshold, K_c = fracture toughness

Since the crack opens during shut down (when stress is tensile at the instrumentation hole edge and combustor is cooling down to room temperature) the propagation is driven by cyclic fatigue only. Static crack growth does not occur.

Walker exponent has been also considered to capture the effect of the mean stress on crack propagation rate, in accordance to the formula below.

$$K_{eff} = \Delta K(1 - R)^{m-1} \quad (10)$$

where: $K_{eff} = K$ equivalent with mean stress effect, $R = K_{max}/K_{min}$, $DK = K_{max}-K_{min}$, $m =$ Walker exponent, $K_{th} =$ crack propagation threshold, $K_c =$ fracture toughness.

The loading input of BHGE tool consists of the stress gradient in the un-cracked model along the crack propagation direction.

This stress gradient is computed using the simplified FE model (20° sector) and running structural analyses for different combinations of input parameters (DP, through thickness temperature gradient, in-plane temperature difference), as already done for the stress model (chapter 7.1).

Also in this case, the stress gradient primarily depends on the distance ‘d’, between the locations at T_{max} and T_{min} . Figure below shows the stress gradient along the axial direction for one typical loading condition at FSFL steady state.

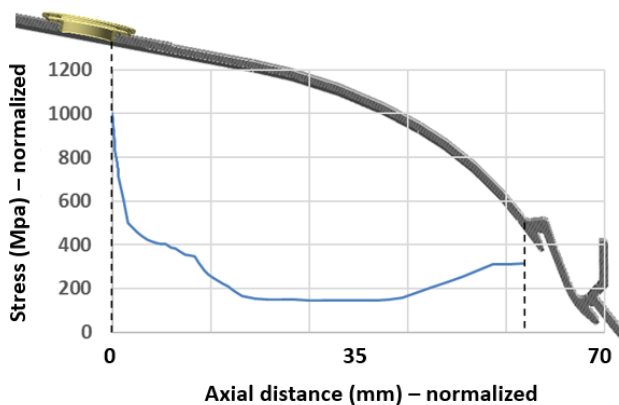


Figure 9. 3. Linear stress gradient in the un-cracked model along the crack propagation direction for a typical operating condition (FSFL SS) – stresses are normalized

Stress gradient decreases very rapidly from instrumentation hole edge towards the liner rear end.

Linear gradients have been converted to elastic plastic gradients, using Glinka method. Some amount of compressive plastic stress around the hole during operation gives tensile residual stresses at machine shut down, which are also captured with the same method.

Once inserted into the BHGE crack growth tool, the stress gradients at operating condition and at shutdown, and the walker exponent are then used to compute the crack propagation rate and define the critical crack length after which a disruptive propagation is expected to occur.

The method used herein is conservative, since crack propagation is load driven (overall load remains constant with growing crack) while the actual structural behavior of the system is thermally (or displacement) driven, (overall load decreases as the crack grows). A further enhancement of the crack propagation model is currently under

development in BHGE, which considers the explicit simulation of the crack in a FE environment. Although conservative, the method proposed herein is however very useful in providing a robust indication of the damage severity, and is also well suited to be incorporated into an automated prognostic tool.

As an example, the figure below shows the crack evolution with the number of cycles for different sets of normalized input parameters at operating conditions, for -3s material properties.

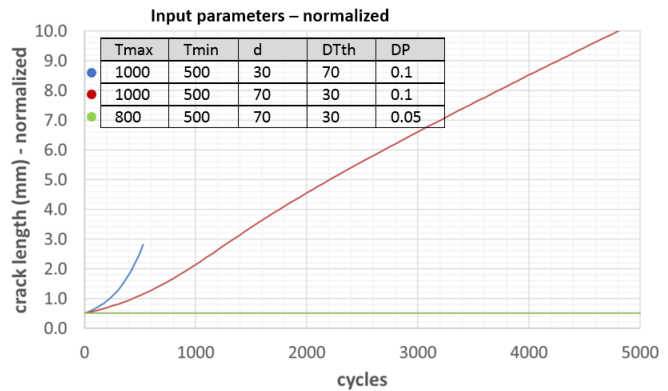


Figure 9.4. Crack propagation rate for different combination of input parameters

As already seen in the stress and LCF models, the in-plane delta temperature and the distance $T_{max}-T_{min}$ have a major impact in the crack propagation rate.

10. APPLICATION TO ACTUAL TRANSIENT MISSION FROM FETT

All the models treated in the previous chapters (thermal, stress, LCF, crack propagation) have been connected together and integrated in a software platform developed in Matlab.

Such a software is capable of producing the life estimation of outer liner at the instrumentation hole in real time, given the actual operating mission profile of the machine.

This enhanced prediction capabilities allowed to capture the physical effects producing a possible failure at the hole and to encircle the operating envelope of the GT for the instrumentation hole to be in the safe zone.

It is also one of the analytical bricks of NovaLT16 digital twin. Once connected to the machine control system or remote diagnostics, and once integrated with component data and field evidences, the model can promptly serve as a next generation predictor within digital twin paradigm.

CONCLUSIONS

A simplified physics based model of the instrumentation hole of NovaLT16 outer liner has been created. The model extracts the global machine operating parameters from the GT control system or remote

diagnostics and uses them as input to compute the outer liner metal temperature distribution.

Metal temperatures are, in turn, elaborated by a simplified stress model, which computes the linear elastic stress at the critical instrumentation hole edge, transforms it into an elastic plastic stress (and stress gradient along the crack propagation direction) through Glinka method and calculates the delta strain for any combination of global input parameters.

Delta strain then enters the LCF life model which is capable of predicting crack nucleation life, while elastic plastic stress gradient is used to calculate the crack growth rate for any given GT mission profile.

This approach is not limited to the specific case analyzed in this study, since it can be easily exportable to other similar physical problems, due to its inherent modularity.

Similarity of the physics and modularity of the platform represent two important aspects to define the field of applicability of the new approach. Generally speaking, the simplified lifing models could be used to accompany the design stages, to solve RCA's, to improve the knowledge of the physical assets, to perform predictive maintenance, all within a novel integrated digital framework, able to respond more promptly to business and market requests.

AKNOWLEDGEMENTS

The authors want to thank BHGE combustion team, Service department and GE Research Center for the support provided during the implementation of NovaLT16 thermal structural modelling of the combustion chamber.

REFERENCES

- [1]. Asti et al., 'Heavy duty gas turbine performance and endurance testing: the NovaLT16 experience', ASME Turbo Expo 2018
- [2]. Cerutti et al., 'Dry Low Nox emissions operability enhancement of a heavy-duty gas turbine by means of fuel burner design development and testing', ASME Turbo Expo 2018
- [3]. M. Knop, R. Jones, L. Molent, C. Wang, 'On the Glinka and Neuber methods for calculating notch tip strains under cyclic load spectra', International Journal of Fatigue, Volume 22, Issue 9, October 2000, Pages 743-755
- [4]. Jesper Kristensen, Isaac Asher, You Ling, Kevin Ryan, Arun Subramaniyan, Liping Wang, 'Predictive analytics with an advanced Bayesian modeling framework', MODSIM World 2017
- [5]. Jablonski, David Albert, 'Fatigue behavior of hastelloy-X at elevated temperatures in air,

- vacuum and oxygen environment', a dissertation from MIT, 1978
- [6]. AH. Lefebvre, DR Ballal, 'Gas Turbine Combustion: Alternate Fuels and Emissions', CRC Press, 3rd Edition
- [7]. G. Leonard and J. Stegmaier, 'Development of an Aeroderivative Gas Turbine Dry Low Emissions Combustion System', Engineering for Gas Turbines and Power, vol. 116, pp. 542-546, 1993
- [8]. Krzysztof Molski, Grzegorz Glinka, 'A method of elastic-plastic stress and strain calculation at a notch root', Materials Science and Engineering, Volume 50, Issue 1, September 1981, pages 93-100
- [9]. Carl Edward Rasmussen and Chris Williams, 'Gaussian Processes for Machine Learning', the MIT Press, 2006
- [10]. L. Samuelsson, Fatigue Analysis, 'The super-Neuber technique for correction of linear elastic FE results', 26th international congress of the aeronautical sciences, ICAS 2008
- [11]. Y. Xiong, M. Dede and M. Moscinski, 'Combustor modeling and design with uncertainties', 48th AIAA / ASME / ASCE / AHS / ASC Structures, Structural Dynamics, and Materials Conference, AIAA Paper 2007-1871, Honolulu, 2007